Polymer Chemistry

Synthetic Mimics of Cyclic Antimicrobial Peptides via Templated Ring-Opening Metathesis (TROM)

Journal:	*Polymer Chemistry*
Manuscript ID	PY-ART-08-2019-001271.R1
Article Type:	Paper
Date Submitted by the Author:	27-Sep-2019
Complete List of Authors:	Zhou, Zhe; Rensselaer Polytechnic Institute, Materials Science and Engineering Ergene, Cansu; Rensselaer Polytechnic Institute, Materials Science and Engineering Palermo, Edmund; Rensselaer Polytechnic Institute, Materials Science and Engineering

Synthetic Mimics of Cyclic Antimicrobial Peptides via Templated Ring-Opening Metathesis (TROM)

Zhe Zhou, Cansu Ergene, Edmund F. Palermo*

Materials Science and Engineering, Rensselaer Polytechnic Institute, 110 8th St., Troy, NY 12180

*email: palere@rpi.edu

ABSTRACT

We utilized a templated ring-opening metathesis (TROM) strategy to synthesize a series of precision macrocyclic olefins, each containing two, three or four repeating units of a cyclooctene with pendant carboxylic acid side chains. The structures were confirmed by a combination of NMR spectroscopy, MALDI, and MALDI ms/ms fragmentation studies. In accordance with previous work, we found that cyclooctene monomers covalently tethered to precision oligo(thiophene)s yield exclusively macrocyclic products when subjected to the Grubbs 3rd generation catalyst in highly dilute solution (10^{-4} M in DCM, 0 °C). Upon hydrolytic liberation of the daughter oligo(olefin) product, further derivatization with cationic groups confers antibacterial and hemolytic activities. We compare the biological activity of these precision macrocycles to that of a polydisperse sample prepared by direct ROM in the absence of a template. Surprisingly, the relatively ill-defined, disperse mixture of oligomeric species exerted biological activity comparable to that of the precision oligomeric macrocycles, suggesting a remarkable degree of tolerance for heterogeneity. These findings provide nuance to the structure-activity relationships understood thus far for AMPs and their mimics, especially in the context of relatively underexplored macrocyclic compounds.

INTRODUCTION

Precision synthesis of macromolecules is a long sought-after target in the chemical sciences; exquisite control of sequence, stereochemistry, and chain length dispersity of macromolecules remain outstanding challenges at the forefront of the field,[1-12] with the ultimate goal to rival or exceed the sophisticated structure and function of naturally-occurring biomacromolecules.

Antimicrobial peptides (AMPs) are a diverse class of biomacromolecules with no particular conserved sequence or secondary structural motif.[13-17] The putatively membrane-disrupting antibacterial activity depends mainly on physiochemical attributes such as cationic charge, hydrophobicity, and short chain length.[18-20] Since the activity is dominated by such physical properties, the stereochemistry plays no role in their bioactivity.[21] As a result, synthetic polymers/oligomers with imperfect control of sequence, stereochemistry, and dispersity have successfully mimicked the physiochemical attributes of AMPs with potent antibacterial activity and minimal toxicity to human cells, despite their inherent chemical heterogeneity.[22-29] These findings appear to suggest that imperfection in synthetic macromolecules is irrelevant to their antibacterial efficacy. On the other hand, it is known that the sequence and dispersity of polymer chains does affect their physiochemical properties, and in turn, thus may impact their biological activity. Indeed, a few studies have shown pronounced sequence effects in synthetic antimicrobial polymers and oligomers.[30-32] To our knowledge, the role of chain length *dispersity* in antibacterial activity has only been directly measured in one study on linear oligomers[33] and has never been studied for cyclic antibacterial agents of any kind.

Cyclic AMPs represent a particularly interesting subset of the class,[34-37] although they represent only a small minority of AMPs. Biophysical experiments and MD simulations have suggested that the antimicrobial cyclic peptide BPC194 has enhanced activity, relative to the

linear variant, due to stronger membrane binding and deeper membrane penetration.[38] Polymyxin B is a notable example of a cyclic cationic/amphiphilic peptide that is clinically used as an antibiotic drug.[39] Interestingly, Polymyxin B is a mixture composed of subtly different polymyxin-type species.[40] Despite their toxicity, polymyxins are still used clinically as antibiotics "of last resort".[41] In contrast to the wealth of literature on linear antibacterial peptides, polymers and oligomers, synthetic mimicry of cyclic antibacterial peptides is currently restricted to just a few known examples.[42-43]

During the course of our research on template-controlled polymerization, we recently discovered a serendipitous method to prepare macrocyclic olefins of defined size.[44] In this template strategy, cyclooctene (COE) monomers are covalently bound to a discrete, monodisperse olio(thiophene) "template" and are then subjected to templated ring-opening metathesis (TROM) with the Grubbs catalyst in dilute solution. The cyclooctene monomers are fully converted to exclusively macrocyclic products with no intra-template metathesis. Then, the cyclic "daughter" oligo(olefin)s are cleaved from the "parent" template via hydrolysis to yield a functional macrocyclic product.

Here, we sought to utilize the recently developed TROM technology to generate functionalized macrocycles that mimic the structure and activity of cyclic AMPs. We successfully prepared a series of olefin macrocycles containing 8×**n** carbon atoms in the ring (with **n** = 2, 3, and 4) and a carboxylic acid functional group handle attached to each repeat unit. Then, we functionalized these side chains with cationic ammonium groups to yield biologically active macrocycles. The cationic and amphiphilic nature of these compounds gave rise to antibacterial activity in the 16-32 μg/mL range, which is typical of a reasonably active antibacterial agent.[22] Interestingly, however, the biological activity appears to be largely

independent of ring size in the range of n = 2, 3, and 4 (macrocycles containing 16, 24, and 32 carbons in the ring). Moreover, an ill-defined heterogeneous mixture of oligomers (with ring size dispersity and linear contaminants) also showed approximately the same antibacterial potency as its individual, unimolecular components. These results show that the present system is rather insensitive to ring size dispersity, with potentially important implications for the scalable and affordable synthesis of AMP-mimetic oligomers and polymers with some inherent and unavoidable degree of chain length dispersity.

RESULTS AND DISCUSSION

Oligomer Synthesis. We prepared a series of oligo(thiophene) templates bearing cycloctene monomers covalently attached to the side chains via ester linkages (denoted as $\mathbf{C_n}$ where **n** = 2, 3, or 4 in Figure 1A), following our previously reported iterative convergent/divergent Stille coupling approach.[44] The details of the synthesis and characterization for these thiophene oligomers and their cyclooctene-functionalized derivatives are given in the supporting information. Each of the monomer-loaded templates was subjected to templated ring-opening metathesis (TROM). To a dilute solution of $\mathbf{C_n}$ (1.5×10^{-4} M, DCM, 0 °C), the Grubbs 3rd generation catalyst (G3) was injected with vigorous stirring. In each case, the catalyst:template ratio was 1:1 such that the catalyst:monomer ratio was 1:**n**. After 1 h, analysis by ^{1}H NMR confirmed that the conversion of cyclooctene monomer to oligomeric product was nearly quantitative. The MALDI spectra showed a single peak with no evidence of intra-template metathesis, *i.e.* "cross-linking", which suggests that the synthetic molecular translation of template to daughter occurred with high fidelity. The isolated TROM product, with oligo(olefin) bound to oligo(thiophene) in a ladder-type architecture, is denoted as $\mathbf{PC_n}$ where n = 2, 3, or 4. Subsequently, the $\mathbf{PC_n}$ substance is hydrolyzed and the resulting daughter oligo(olefin) is

isolated for further derivatization with Boc-protected aminoethanol. The final step is Boc deprotection in TFA to afford the target structures: cationic and amphiphilic macrocycles each containing precisely **n** cationic ammonium groups.

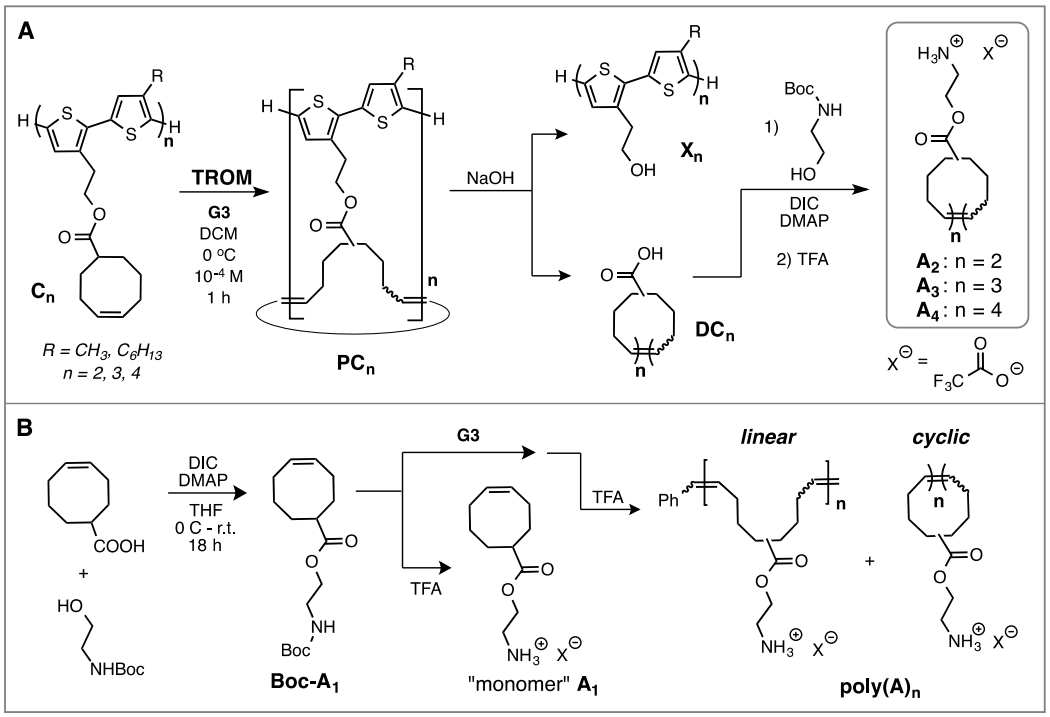

Figure 1. (A) Synthesis of macrocyclic olefins by templated ring-opening metathesis (TROM), hydrolytic liberation of the daughter oligomer, and subsequent functionalization of the daughter to give cationic, amphiphilic macrocycles of defined size. (B) Non-templated control reactions for synthesis of the monomeric compound $\mathbf{A_1}$ and the disperse mixture poly($\mathbf{A_n}$) as control samples for comparison.

We also prepared control samples for comparison (Figure 1B). The "monomer" $\mathbf{A_1}$ was prepared by direct functionalization of the cyclooctene. A heterogeneous mixture of oligomers poly($\mathbf{A_1}$) was prepared by treating Boc-protected $\mathbf{A_1}$ with G3 in the same conditions as used for TROM (1.5×10^{-4} M in DCM, 0 °C, monomer:catalyst = 3:1) but without any template to control the metathesis reactions. Due to the high catalyst loading and dilute conditions, we expected to obtain mostly very short cyclic oligomers of comparable size to the pure compounds $\mathbf{A_2}$, $\mathbf{A_3}$, and

$\mathbf{A_4}$. Indeed, upon TFA deprotection, the resultant sample poly($\mathbf{A_1}$) is a disperse mixture of cationic and amphiphilic oligomers, as confirmed by mass spectroscopy.

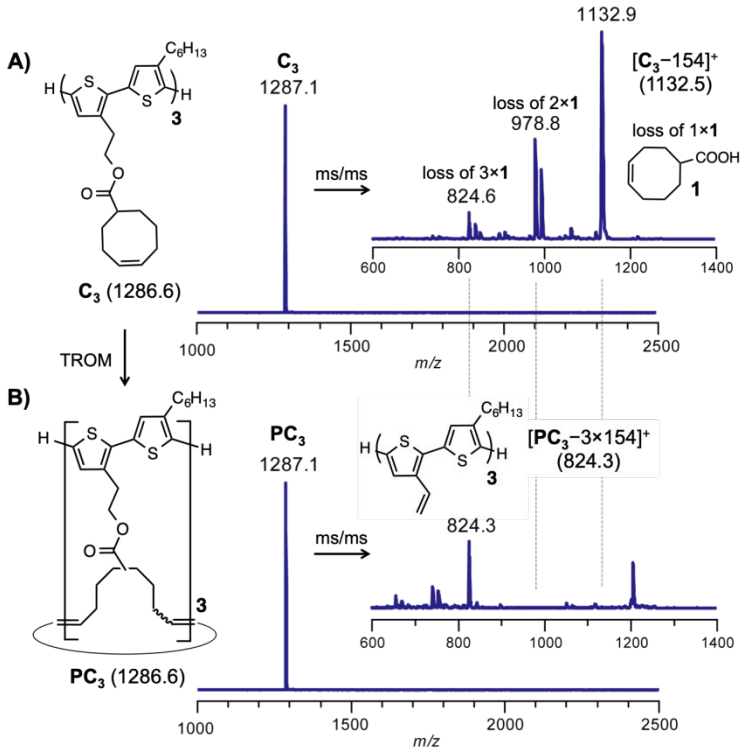

Figure 2. MALDI spectra of (A) C_3 and (B) PC_3 and their respective ms/ms fragmentation patterns (insets).

The MALDI data for each $\mathbf{C_n}$ and $\mathbf{PC_n}$ exhibit a single sharp peak at the expected mass, *e.g.* $\mathbf{C_3}$ and $\mathbf{PC_3}$ are shown in Figure 2. The raw data for all examples in the study are given in the supporting information. Quantitative conversion was confirmed by ^{1}H NMR, in each case, and there was no evidence of any intra-template metathesis (no peak in MALDI at [M]×2) under these previously optimized conditions. Importantly, for each value of **n**, the exact mass before and after TROM appear at the same value of m/z in the MALDI despite full monomer conversion. This observation suggests that the $\mathbf{PC_n}$ products are exclusively macrocyclic and thus contain none of the usual styrenic end groups that are typically expected in the case of conventional ROMP with G3. Compelling evidence to support this hypothesis was gleaned from

MALDI ms/ms fragmentation. The monomer-loaded template $\mathbf{C_3}$, for example, fragments via multiple McLafferty rearrangements to produce peaks corresponding to the molecular ion minus one, two, and three cyclooctene monomers (Figure 2A, inset). In contrast, the fragmentation pattern for $\mathbf{PC_3}$ shows only one such McLafferty fragmentation peak, corresponding to the molecular ion minus *all three* equivalents of monomer (Figure 2B, inset). The lack of any fragments corresponding to loss of just one or two cyclooctene (COE) monomers is clearly consistent with the proposed macrocyclic product structure. This result is in agreement with our previous TROM study. It was initially surprising that a macrocyclic daughter olefin should form in this manner because it must require the ruthenium-bound ω terminus to cross onto the styrenic α terminus, the latter of which is normally considered metathesis-inert. However, the proximity of these groups on the template and the presence of weakly coordinating ester groups might alter reactivity in unanticipated ways. Further, all steps in the TROM process are reversible in principle, but the *only* step in which the catalyst is detached from the template, whereupon it may diffuse away in dilute solution, is the final RCM step. Thus, even if not thermodynamically favored, this ring-closed product may be a kinetically-trapped state.[44] Regardless of the mechanism, however, we obtained exclusively macrocyclic products, in all cases, unambiguously.

Following hydrolytic liberation of the carboxylic acid-functional daughter oligo(olefin)s $\mathbf{DC_n}$ from the parent oligo(thiophene)s $\mathbf{X_n}$, we then endeavored to functionalize these discrete macrocycles with Boc-protected amino ethyl alcohol via standard carbodiimide coupling methods. Finally, deprotection in neat TFA yielded the cationic and amphiphilic macrocyclic target compounds, $\mathbf{A_n}$ (n = 2, 3, and 4). For each case, the products are exclusively cyclic, discrete, monodisperse compounds. A single major peak for each of these cyclic oligomers

appears at the expected m/z value in mass spectra (Figure 3A) and the ^{1}H and ^{13}C NMR spectra are in accord with the proposed structures (supporting information). In each case, the $\mathbf{A_n}$ molecular ions were observed with one amino group protonated and the remainder as neutral amines. Thus, the TROM process enables access to discrete macrocyclic compounds of defined ring size (16, 24, and 32 carbons) with pendant functional groups in the side chains. The primary amine groups, which are largely protonated at physiological pH, combined with the hydrophobic all-carbon backbone of the macrocycles, are expected to endow these molecules with antibacterial activity.

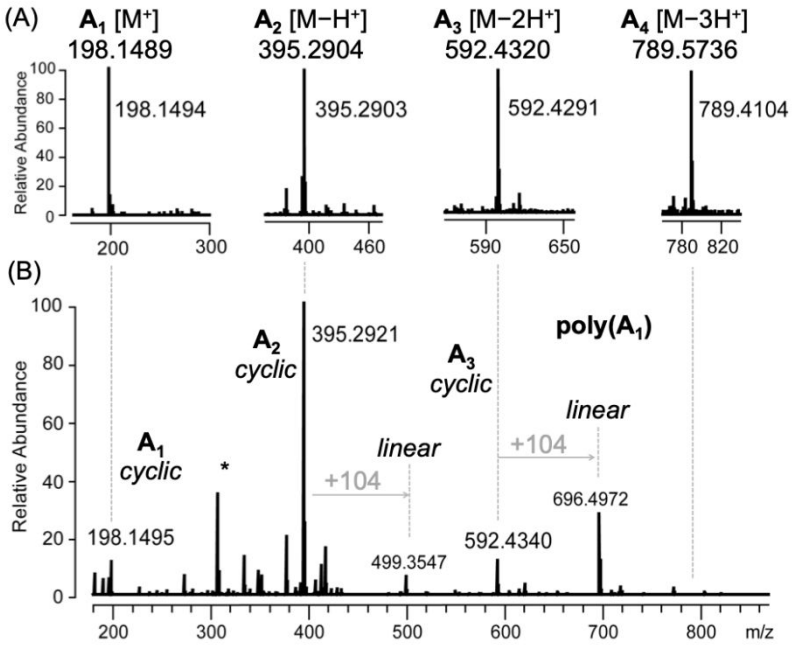

Figure 3. ESI HRMS for (A) the monomer $\mathbf{A_1}$ and the discrete macrocyclic compounds $\mathbf{A_n}$ (**n** = 2, 3, 4) obtained by the TROM process, compared to (B) the disperse mixture of cyclic and linear oligomers formed by non-templated ROM. The * denotes a peak at 307 m/z, which is likely a fragment of the plasticizer DIDP, a commonly observed contaminant in mass spectroscopy.

Examination of poly($\mathbf{A_1}$) by ESI ms revealed that the mixture contains macrocyclic $\mathbf{A_1}$, $\mathbf{A_2}$ (major) and $\mathbf{A_3}$ as well as the linear variants of $\mathbf{A_2}$ and $\mathbf{A_3}$ with styrenic (+104 m/z) end groups derived from the G3 catalyst (Figure 3B). Interestingly, the dimer $\mathbf{A_2}$ is predominately cyclic

with only a minor linear peak; but the trimer **A_3** conversely showed a preference for the linear product over the cyclic analog. Whereas the mechanism is unclear at present, it is reasonable to speculate that the back-biting metathesis reaction required to produce a cyclic oligomer is sensitive to chain length, perhaps because of the steric factors that dictate chain conformations in dilute solution.

We examined the chemical stability of the daughter oligomers in aqueous solution (see ESI Figure S38), since 2-aminoethyl esters may undergo pH-dependent isomerization to the corresponding hydroxyethyl amides. These compounds are stable in neutral aqueous buffers (PBS pH 7.4) at 37 °C for 24 hours, but they isomerize in basic conditions (aq. K_2CO_3, pH 10). Thus, in the assay conditions studied here, the daughter oligomers appear to be chemically unaltered.

Biological Activity. With our cationic and amphiphilic macrocyclic oligomers in hand, we proceeded to evaluate their antibacterial and hemolytic activities *in vitro* (Figure 4). Antibacterial activity is reported as the minimum inhibitory concentration (MIC), *i.e.* the lowest concentration of compound, among a series of serial two-fold dilutions, which completely inhibits the growth of *E. coli* in nutrient-rich media (with a starting inoculum of 10^6 CFU/mL). The MIC values are determined based on the optical turbidity of the media at each concentration ($OD_{600} < 0.01$ for all concentrations at or above MIC). It is important to note that *lower* values of MIC imply a *more potent* antibacterial activity. The characteristic hemolytic concentration (HC_{50}) is defined as the concentration of compound that induces 50% release of hemoglobin from red blood cells in phosphate-buffered saline solution. Lower HC_{50} values are associated with toxic compounds.

Here, we show the HC_{50} values extracted from curve fitting to the Hill equation whereas the full dose-response data and their corresponding curve fits are given in the ESI (Figure S32).

The small molecule monomer $\mathbf{A_1}$, which contains a single cationic ammonium group attached to one hydrophobic cyclooctene unit, was relatively inactive against both bacteria and red blood cells. The MIC value (500 μg/mL) and HC_{50} value (520 μg/mL) of $\mathbf{A_1}$ indicate that this compound is not a very potent antibacterial agent and is rather non-hemolytic. However, when the number of cationic and amphiphilic repeat units in the macrocycle is increased by a single unit, there is a dramatic enhancement of both antibacterial and hemolytic potency. The dimer $\mathbf{A_2}$ exerted both good antibacterial activity (MIC = 16 μg/mL), typical of an AMP, but with comparably strong hemolytic toxicity (HC_{50} = 43 μg/mL). The ratio of HC_{50}/MIC is a commonly used metric to assess the cell-type selectivity of a putatively membrane-disrupting antibacterial agent. For the case of $\mathbf{A_2}$, this value is a modest factor of 2.7×, which is considered weak selectivity. Thus, the compound is categorized as a biocidal agent that almost indiscriminately lyses both bacterial and mammalian cell membranes. Surprisingly, the compounds $\mathbf{A_3}$ (MIC = 21 μg/mL, HC_{50} = 60 μg/mL) and $\mathbf{A_4}$ (MIC = 20 μg/mL, HC_{50} = 95 μg/mL) showed rather similar biocidal activity as compared to $\mathbf{A_2}$. In all cases, the MIC and HC_{50} are on the same order of magnitude. The tetramer $\mathbf{A_4}$ is just slightly more cell-type selective (HC_{50}/MIC ~ 4.8) relative to the dimer, and both are categorically biocidal agents.

Note that the MIC values indicate the inhibition of growth, but do not prove that cells were *killed*. Thus, we also checked the minimum bactericidal concentration (MBC) by withdrawing an aliquot from the microplate at the MIC and streaking onto MH agar. In each case, the MBC was either equal to the MIC, or just one dilution higher, which confirms that these compounds are indeed bactericidal and not solely bacteriostatic *in vitro*.

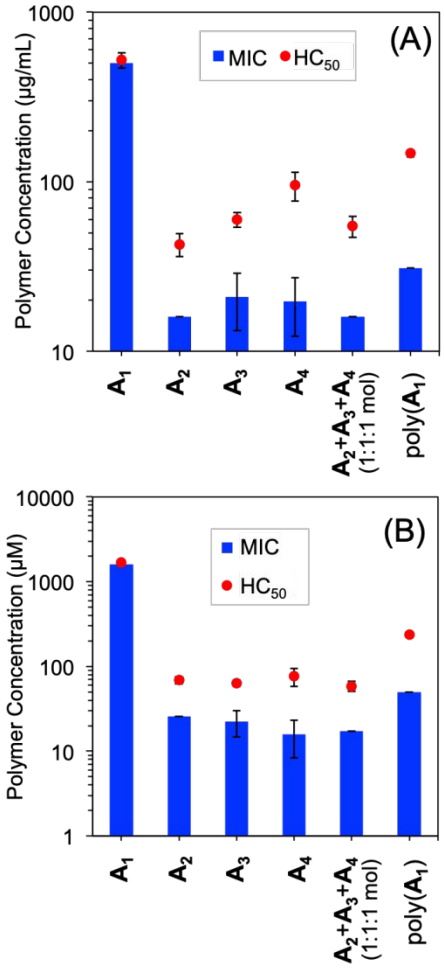

Figure 4. MIC against *E. coli* and HC_{50} against red blood cells for the macrocylic compounds in this study, expressed in units of (A) μg/mL and (B) μM. The discrete compounds (**A_1**, **A_2**, **A_3**, and **A_4**) are directly compared to two heterogeneous mixtures: the equimolar mixture of **A_2**, **A_3**, and **A_4** (the "artificially" disperse sample) as well as poly(**A_1**) obtained via non-templated ROM of **Boc-A_1** in dilute solution. The poly(**A_1**) sample contains a mixture of A_1, A_2, A_3 as well as the linear analogs of A_2 and A_3 with styrene end groups. Data are the average of 3 trials performed in triplicate (n =9). Error bars represent the standard deviation.

We reported antibacterial and hemolytic activity above in units of μg/mL concentration (Figure 4A). Since these compounds substantially differ in molecular weight, it is also informative to express these activities in units of μM, which is more indicative of the inherent activity of individual molecules as opposed to the mass-based μg/mL units. When the data are plotted in units of μM (Figure 4B), the similarity in activity becomes even more pronounced. The HC_{50} values for each **A_n** compound from **n** = 2−4 are all in the narrow range of 59−76 μM,

which suggests nearly identical activity per individual molecule. The MIC values for these same three compounds are also nearly identical, within the narrow range of 16−26 μM. It is apparent that the macrocycles, with **n** = 2 − 4, all exhibit antibacterial and hemolytic activity that is largely independent of ring size, contrary to our expectations.

It is rather atypical in the field of AMP-mimetic oligomers to find that the biological activity does not depend on the degree of oligomerization. To shed light on these unexpected results, we carried out the same bioassays for the control sample **poly(A_1)**, a disperse mixture of cyclic and linear oligomers of varying chain length. Remarkably, this ill-defined heterogeneous population exerts antibacterial and hemolytic activities (MIC = 31 μg/mL, HC_{50} = 148 μg/mL) that are only slightly less active than the discrete, unimolecular compounds prepared by the TROM method. Given this outcome, we then prepared an artificially disperse sample by mixing solutions of $\mathbf{A_2}$, $\mathbf{A_3}$ and $\mathbf{A_4}$ in 1:1:1 equimolar ratios. This well-defined sample has the same number-average molecular weight as $\mathbf{A_3}$ (M_n = 933.6 g/mol) but the mixture has some dispersity (Đ = 1.07). This sample exerted biological activity (MIC_{mix} = 16 μg/mL, $HC_{50,mix}$ = 55 μg/mL) almost identical to that of $\mathbf{A_3}$.

We find that the antibacterial and hemolytic activities of the 1:1:1 defined mixture are well predicted by the inverse average (Ruess average) of the individual component activities, as in equation (1).

$$\frac{1}{MIC_{mix}} \approx \frac{1}{MIC_{\text{Reuss}}} = \sum \frac{f_i}{MIC_i} = \frac{1/3}{MIC_{A2}} + \frac{1/3}{MIC_{A3}} + \frac{1/3}{MIC_{A4}}, \qquad (1)$$

where MIC_i is the MIC value of the i^{th} component in the mixture and f_i is the molar fraction of that component. The reason for using an inverse averaging technique is that the *activity* of the compound is inversely related to the MIC value. For example, a hypothetical 1:1 mixture of X, a potent antibacterial (MIC_X = 1 μg/mL), with Y, an inactive substance (MIC_Y = 1000 μg/mL),

would have activity approximately ½ as potent as pure X ($MIC_{X/Y,mix} \approx 2$ μg/mL). In other words, the inactive Y *dilutes* the potent activity of X by a factor of 2. The simple average of MIC values would incorrectly predict an MIC of ~500 μg/mL, on the other hand.

The summation for the case of our equimolar, three-component mixture is given in equation (1), above. When the MIC values for $\mathbf{A_2}$, $\mathbf{A_3}$, and $\mathbf{A_4}$ are entered, this averaging technique returns a predicted MIC_{mix} value of 19 μg/mL, which is very close to the experimental value of 16 μg/mL. The same method predicts an $HC_{50,mix}$ of 59 μg/mL, which is very close to the experimental value of 55 μg/mL. It is not straightforward to calculate the average for poly($\mathbf{A_1}$) because this sample contains linear oligomers of unknown activity in their pure form. If one performs the calculation ignoring the presence of these linear contaminants, the resulting prediction is off by a factor of 3, which might imply that the styrene-containing linear components of the mixture do have a significant impact on the activity of the disperse sample.

The extent to which chain length dispersity plays a role in the antibacterial and hemolytic activities of AMPs, and their mimics, has not been firmly established in the literature. AMPs are diverse in sequence and secondary structure, but share common physiochemical characteristics: cationic charge, hydrophobicity and relatively short chain length. Whereas AMPs are typically monodisperse, the vast majority of synthetic polymers made to mimic their physiochemical characteristics possess chain length dispersity. Even the most controlled methods of synthetic polymerization, which can give $Đ < 1.1$, still give rise to populations that contain a broad range of chain lengths as compared to unimolecular peptides. Nevertheless, these synthetic methods have yielded numerous examples of polymers with MIC and HC_{50} values that rival or surpass the efficacy of AMPs, even in cases with Đ as high as 1.5 for polymethacrylates.[45] In addition, the clinically used drug polymyxin B (a cyclic, cationic, amphiphilic peptide) is a mixture of

biomolecules with subtle structural differences. These findings would seem to indirectly suggest that dispersity is not universally a key determinant of antibacterial activity.

In a recent study on photodynamic antibacterial oligo(thiophene)s, we did a direct comparison which clearly showed that dispersity plays a significant role in determining the antibacterial and hemolytic activities.[33] Here, we find that dispersity plays almost no role as an activity determinant. Although these results might seem contradictory, in both cases the activity obeyed the Reuss average of the components (lower-bound rule of mixtures). The generalizable principle is thus: if a heterogeneous mixture is composed of individual components that have similar activity, then dispersity will play little or no role in dictating the activity of the mixture. Conversely, if a mixture is composed of individual components that have dramatically different activity, then dispersity will play a key role in dictating the activity of the mixture. The compounds in the present study fall into the former category, whereas the compounds studied previously fell into the latter category. The extent to which dispersity "matters" in the design of antibacterial agents will therefore depend on whether the individual components within the mixture each possess similar or distinct activities as compared to one another. If it is confirmed that the sub-populations within a disperse mixture have similar activity individually, then some extent of dispersity will likely be tolerated in that particular system. In such cases, one may confidently proceed to utilize a more scalable and affordable method of synthesis that does not require perfectly homogeneous macromolecular structure.

Confocal Microscopy. The MIC value of an antibacterial agent demonstrates activity in terms of *inhibition of growth*, but does not strictly show cell death. In order to probe the bactericidal activity of the macrocyclic oligomers in this study, we employed a LIVE/DEAD stain assay.

This procedure involves a green dye (SYTO9) that stains both live and dead *E. coli* cells and a red dye (propidium iodide, PI), which only emits upon intercalation with DNA inside the bacterial cell. PI staining implies that the cells have permeabilized membranes, since healthy cell membranes are PI-impermeable. Still, it is important to emphasize that PI staining does not prove that the *cause* of death was membrane permeabilization *per se*. It is possible that cells could perish by some other mechanism and then lose their membrane integrity as a byproduct of cell death rather than a root cause. The details of the antibacterial mechanism exerted by these compounds remain to be explored in depth. Given their cationic and amphiphilic structure, however, the simplest explanation for the bactericidal activity observed here is that the surfactant-like molecules permeabilize bacteria cell membranes, which ultimately leads to cell death.

The control *E. coli* sample in PBS, with no antibacterial agent present, showed only emission from the green channel with no detectable red signal (Figure 5A-C). When exposed to either $\mathbf{A_2}$ or $\mathbf{A_4}$, on the other hand, the cells emit strongly in the red, consistent with PI-staining and thus indicative of cell death. The overlaid images (Figure 5 F and I) show a high degree of overlap between the green and red signals, such that the majority of E. coli cells appear yellow in color. Taken together, these observations are all consistent with the notion that $\mathbf{A_2}$ and $\mathbf{A_4}$ indeed kill bacteria cells, in addition to their ability to inhibit growth.

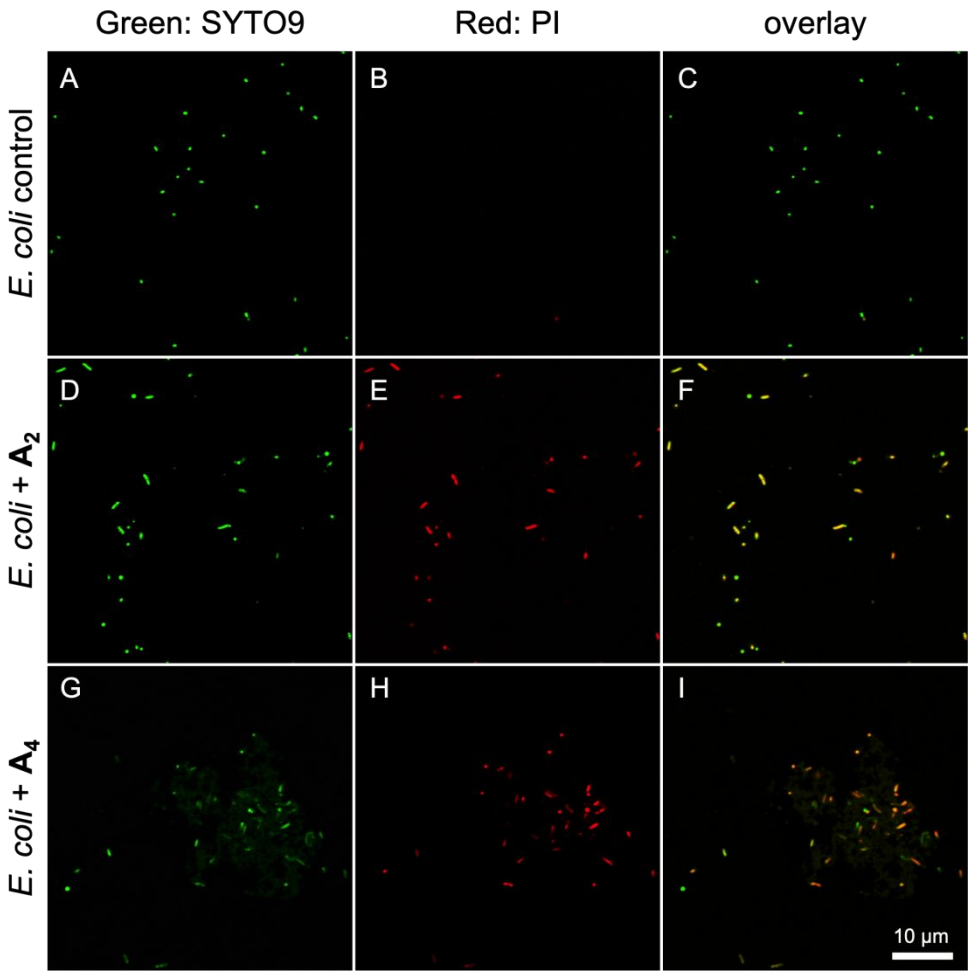

Figure 5. LIVE/DEAD stained *E. coli* in the absence of antibacterial agents (A-C) and in the presence of $\mathbf{A_2}$ (D-F) and $\mathbf{A_4}$ (G-I) at a concentration of 2×MIC. The green channel is STYO9 (A,D,G), which stains both live and dead bacteria, the red channel is propidium iodide (PI), which only emits when intercalated to DNA inside the bacteria cells (B,E,H) and the third column contains an overlay of the first two.

Interestingly, there are subtle differences in the appearance of *E. coli* cells exposed to $\mathbf{A_2}$ versus $\mathbf{A_4}$. In Figure 5D, it is clear that each *E. coli* cell is individually-suspended in the planktonic state with $\mathbf{A_2}$ present. The red channel shows that each of these cells has been permeabilized, but the cells still retain their characteristic size and shape. In contrast, Figure 5H reveals that the cells treated with $\mathbf{A_4}$ are more clustered into an aggregated state. Between the individual cells, it is clear that some diffuse green emission is present. The cells do not all retain their characteristic size and shape, with some green-stained material apparently lacking the familiar cellular structure altogether. These observations may be the result of cellular debris

produced by surfactant-like lysis of the bacterial membranes or aggregates of **A_4** with some cellular components. Although the MIC and HC_{50} values of these two compounds are very similar, it would appear that the details of their interactions with bacterial cells are not identical. From these images, it seems that **A_4** works by a mechanism that involves aggregation of cells and surfactant-like lysis whereas **A_2** exerts its effect on cells individually in solution. The latter mechanism is considered more desirable because gross membrane lysis can release toxic substances and lead to sepsis.

CONCLUSIONS

We reported the first synthesis of several novel, well-defined macrocyclic olefins bearing cationic ammonium side chains, by elaboration of our previously reported templated ring-opening metathesis (TROM) method. The success of the synthetic approach was rigorously confirmed by a combination of MALDI, ms/ms, and ESI HRMS with ^{1}H and ^{13}C NMR spectroscopy. In each case, exclusively cyclic products are formed, which was not predicted *a priori* based on established knowledge of G3 reactivity. We ascribe this unusual catalyst behavior to the local immobilization and proximity of multiple monomer units on a rigid template molecule dissolved in very highly dilute solution. Upon hydrolytic removal of the daughter olefin from the parent template molecule, we isolated and functionalized these precision macrocycles. Installation of primary amine groups, which are cationic by virtue of protonation at physiological pH, in the side chains endows these cyclic compounds with antibacterial and hemolytic activity. Surprisingly, we found that the ring size (in the range of 16-32 carbons) did not significantly impact the observed activity. Moreover, a heterogeneous mixture of oligomeric species also showed quite similar results. Thus, in this particular system,

we find that the dispersity of molecular size is not a key determinant of biological activity, in stark contrast to previous findings. These seemingly contradictory results are unified, however, by the understanding that disperse populations will exhibit activity as predicted by the Reuss average of the MIC (or HC_{50}) values for the individual components within the mixture. Thus, a disperse sample that is composed of molecules with similar activity was correctly predicted to display the same activity as the pure components. On the other hand, if there exist subpopulations with substantially different activity, then dispersity is expected to play a key role as a determinant of biological activity. In that light, the extent to which antibacterial polymers/oligomers can tolerate dispersity without compromising activity is likely to vary across different classes of materials. The question as to whether a discrete, unimolecular compound (well defined but more labor intensive and costly) is inherently better than a disperse population (less perfectly defined but more scalable and cost-effective) will require judicious consideration of individual components.

EXPERIMENTAL METHODS

General Synthetic Procedures. Synthesis of oligo(thiophene) templates and TROM were done according to our previous report.[44] Information on reagents and instrumentation, detailed experimental procedures, and all characterization data are given in the Supporting Information. General protocols of synthesizing cyclic AMP-mimic oligomers are described below.

Hydrolysis. Excess potassium hydroxide (1M in H_2O) was added into template molecules DMF solution and stirred vigorously at 55 °C for 48 hours. The solvent was removed under vacuum and the residue was subjected to 10mL 1M KOH and 10ml ethyl acetate. The water phase was collected and 1M HCl solution was added until pH > 7. The solution was diluted with

ethyl acetate and washed with water. Organic layer was dried over sodium sulfate, filtered, and concentrated under reduced pressure. The product was obtained without further purification.

Esterification. In an oven-dried Schlenk flask, the cyclooctene monomer with carboxylic acid group (1 equiv) and N-(tert-Butoxycarbonyl)ethanolamine (1.5 equiv) were dissolved in anhydrous DCM under nitrogen and DMAP (0.1 equiv) was added in one portion. The solution was cooled to 0 °C and stirred for 10 min before injection of neat DIC (2 equiv). The reaction mixture was allowed to warm to room temperature and stirred overnight. The organic layer was concentrated under reduced pressure. The crude product was purified by silica gel chromatography.

BOC Deprotection. Excess TFA solution was added to the product and stirred for 1 hour. Then TFA was evaporated and the residue was washed with diethyl ether three times to yield pure product.

Antibacterial assays. The *in vitro* minimum inhibition concentration (MIC) of cyclic antimicrobials was assessed. Oligomer stock solutions were prepared in 50% DMSO-50% of 0.01% acetic acid-deionized H_2O with 2-fold serial dilutions of the stock, starting from 5 mg/ml to 0.15 μg/ml. A single colony of *Escherichia coli* ATCC 25922 was inoculated in Muller-Hinton (MH) broth at 37 °C in shaking incubator overnight. The turbid dilution was diluted to OD_{600} = 0.1 (measured by Molecular Devices SpectraMax M2), regrown for 90 min to midlogarithmic phase (OD_{600} = 0.5 – 0.6) in MH broth. It was diluted to OD_{600} = 0.001 in MH broth, corresponding to ~5 x 10^5 cfu/ml based upon colony counting on MH agar plates. The bacterial suspension (90 μl) was mixed with each polymer concentration (10 μl) in a sterile 96-well round-bottom polypropylene microplate (Chemglass #229590) and wrapped with parafilm. The microplate was incubated for 16 hours at 37 °C. MIC was defined as the lowest

concentration of polymer, which inhibits visible cell growth. Each compound was tested three times in triplicate. Final MIC values were determined by the average MIC of multiple tests. As a negative control, stock solution of DMSO in 0.01% acetic acid-deionized H_2O was prepared in microplates with 2-fold serial dilutions, starting from 5% (v/v) and tested as oligomers.

Hemolysis assays. Hemolytic activity of cyclic antimicrobials was determined by hemoglobin release assay using the same oligomer stock solutions for MIC assays. 1 ml of 10% (v/v) suspension of sheep red blood cells (MP Biomedicals) was centrifuged at 2000 rpm for 3 min and washed with PBS of pH 7.4. The RBCs were washed with PBS two more times. The resulting stock was diluted 10-fold in PBS to provide 1% (v/v) RBC assay stock. In a sterile 96-well round-bottom polypropylene microplate, 90 μl of 1% (v/v) RBC assay stock was mixed with 10 μl of each of the oligomer dilution. PBS is used as a negative control. Triton X-100 was used as a positive control 0.1% (v/v) for complete lysis. Microplate was wrapped with parafilm, secured in orbital shaker at 37 °C and incubated at 200 rpm for 60 min. The microplate was centrifuged at 1000 rpm for 10 min. In another sterile microplate, 10 μL of supernatant was diluted in 90 μl PBS. The absorbance at 415 nm was recorded using a microplate reader. Hemolysis was plotted as a function of polymer concentration and the hemolysis fraction. HC_{50} was described as the polymer concentration causing 50% hemolysis relative to the positive control. This value was estimated by the fitting to the Hill equation, $H([P]) = 1/(1+(HC_{50}/[P])^n)$ where H is the hemolysis fraction ($H = [OD_{415}(\text{polymer}) - OD_{415}(\text{buffer})] / [OD_{415}(\text{TritonX}) - OD_{415}(\text{buffer})]$), [P] is the oligomer concentration, n and HC_{50} are variable parameters for curve fitting. Each compound was tested three times in triplicate. The % hemolysis values from each trial were averaged and then the HC_{50} was calculated from the curve fitting.

Confocal Microscopy. A single colony of *Escherichia coli* ATCC 25922 was inoculated in Muller-Hinton broth at 37 °C in shaking incubator overnight. The turbid suspension was diluted to OD_{600} = 0.1, regrown for 90 min to mid-logarithmic phase (OD_{600} = 0.5 – 0.6) in MH broth. Resulting suspension was centrifuged at 2000 rpm for 5 min and the supernatant was carefully discarded by pipetting. Collected bacteria in centrifuge tube were resuspended in PBS of pH 7.4. The bacterial suspension was diluted to OD_{600} = 0.1 (~$5x10^7$ cells/ml) in PBS. Compound solution (200 μg/ml in 2% (v/v) DMSO-PBS) was added into 4 ml of bacterial suspension to provide the final concentration of 40 μg/ml (~2×MIC). Suspension was incubated at 37 °C for 180. After incubation, cells were stained with BacLight™ Bacterial Viability Kit L-7007 (equal volumes of Component A and Component B) and incubated at room temperature for 15 min in dark. 5 μl of dyed bacterial suspension was placed on Nunc™ glass bottom dish (Thermo Fisher Scientific) and covered with glass cover slip. Cells were visualized under laser scanning confocal microscopy using Argon and HeNe1 lasers. SYTO9 (green dye) stain both live and dead cells, but PI (red dye) stains just dead cells. Same procedure above was applied for negative control with *E. coli* (final concentration of DMSO in PBS: 0.4%).

ACKNOWLEDGEMENTS

The authors gratefully acknowledge Dr. Dmitri Zagorevski for assistance with mass spectroscopy and helpful discussions. This work was supported in part by the Army Research Office STIR Grant #66992-CH-II and the NSF CAREER Award # 1653418.

REFERENCES

1. Badi, N.; Lutz, J. F., Sequence control in polymer synthesis. *Chem Soc Rev* **2009,** *38* (12), 3383-3390.
2. Lutz, J. F., Sequence-controlled polymerizations: the next Holy Grail in polymer science? *Polym Chem* **2010,** *1* (1), 55-62.
3. Lutz, J.-F.; Ouchi, M.; Liu, D. R.; Sawamoto, M., Sequence-Controlled Polymers. *Science* **2013,** *341* (6146), 628.
4. Kamigaito, M.; Ando, T.; Sawamoto, M., Metal-catalyzed living radical polymerization. *Chem Rev* **2001,** *101* (12), 3689-3745.
5. Hibi, Y.; Tokuoka, S.; Terashima, T.; Ouchi, M.; Sawamoto, M., Design of AB divinyl "template monomers" toward alternating sequence control in metal-catalyzed living radical polymerization. *Polym Chem* **2011,** *2* (2), 341-347.
6. Hibi, Y.; Ouchi, M.; Sawamoto, M., Sequence-Regulated Radical Polymerization with a Metal-Templated Monomer: Repetitive ABA Sequence by Double Cyclopolymerization. *Angew Chem Int Edit* **2011,** *50* (32), 7434-7437.
7. Hibi, Y.; Ouchi, M.; Sawamoto, M., A strategy for sequence control in vinyl polymers via iterative controlled radical cyclization. *Nat Commun* **2016,** *7*.
8. Kamigaito, M.; Satoh, K., Stereospecific living radical polymerization for simultaneous control of molecular weight and tacticity. *J Polym Sci Pol Chem* **2006,** *44* (21), 6147-6158.
9. Satoh, K.; Kamigaito, M., Stereospecific Living Radical Polymerization: Dual Control of Chain Length and Tacticity for Precision Polymer Synthesis. *Chem Rev* **2009,** *109* (11), 5120-5156.
10. Braunecker, W. A.; Matyjaszewski, K., Controlled/living radical polymerization: Features, developments and perspectives. *Prog Polym Sci* **2008,** *33* (1), 165-165.
11. Weiss, R. M.; Short, A. L.; Meyer, T. Y., Sequence-Controlled Copolymers Prepared via Entropy-Driven Ring-Opening Metathesis Polymerization. *ACS Macro Lett* **2015,** *4* (9), 1039-1043.
12. Gentekos, D. T.; Dupuis, L. N.; Fors, B. P., Beyond Dispersity: Deterministic Control of Polymer Molecular Weight Distribution. *J Am Chem Soc* **2016,** *138* (6), 1848-1851.
13. Zasloff, M., Antimicrobial peptides of multicellular organisms. *Nature* **2002,** *415* (6870), 389-395.
14. Brogden, K. A.; Ackermann, M.; McCray, P. B.; Tack, B. F., Antimicrobial peptides in animals and their role in host defences. *Int J Antimicrob Ag* **2003,** *22* (5), 465-478.
15. Brogden, K. A., Antimicrobial peptides: Pore formers or metabolic inhibitors in bacteria? *Nat Rev Microbiol* **2005,** *3* (3), 238-250.
16. Fjell, C. D.; Hiss, J. A.; Hancock, R. E. W.; Schneider, G., Designing antimicrobial peptides: form follows function. *Nat Rev Drug Discov* **2012,** *11* (1), 37-51.
17. Matsuzaki, K., Magainins as paradigm for the mode of action of pore forming polypeptides. *BBA-Rev Biomembranes* **1998,** *1376* (3), 391-400.
18. Wang, Z.; Wang, G. S., APD: the Antimicrobial Peptide Database. *Nucleic Acids Res* **2004,** *32*, D590-D592.
19. Wang, G. S.; Li, X.; Wang, Z., APD2: the updated antimicrobial peptide database and its application in peptide design. *Nucleic Acids Res* **2009,** *37*, D933-D937.
20. Wang, G. S.; Li, X.; Wang, Z., APD3: the antimicrobial peptide database as a tool for research and education. *Nucleic Acids Res* **2016,** *44* (D1), D1087-D1093.

21. Won, A.; Khan, M.; Gustin, S.; Akpawu, A.; Seebun, D.; Avis, T. J.; Leung, B. O.; Hitchcock, A. P.; Ianoul, A., Investigating the effects of L- to D-amino acid substitution and deamidation on the activity and membrane interactions of antimicrobial peptide anoplin. *Bba-Biomembranes* **2011,** *1808* (6), 1592-1600.
22. Ergene, C.; Yasuhara, K.; Palermo, E. F., Biomimetic antimicrobial polymers: recent advances in molecular design. *Polym Chem* **2018,** *9* (18), 2407-2427.
23. Konai, M. M.; Bhattacharjee, B.; Ghosh, S.; Haldar, J., Recent Progress in Polymer Research to Tackle Infections and Antimicrobial Resistance. *Biomacromolecules* **2018,** *19* (6), 1888-1917.
24. Tew, G. N.; Liu, D. H.; Chen, B.; Doerksen, R. J.; Kaplan, J.; Carroll, P. J.; Klein, M. L.; DeGrado, W. F., De novo design of biomimetic antimicrobial polymers. *P Natl Acad Sci USA* **2002,** *99* (8), 5110-5114.
25. Arnt, L.; Tew, G. N., New poly(phenyleneethynylene)s with cationic, facially amphiphilic structures. *J Am Chem Soc* **2002,** *124* (26), 7664-7665.
26. Kuroda, K.; DeGrado, W. F., Amphiphilic polymethacrylate derivatives as antimicrobial agents. *J Am Chem Soc* **2005,** *127* (12), 4128-4129.
27. Mowery, B. P.; Lee, S. E.; Kissounko, D. A.; Epand, R. F.; Epand, R. M.; Weisblum, B.; Stahl, S. S.; Gellman, S. H., Mimicry of antimicrobial host-defense peptides by random copolymers. *J Am Chem Soc* **2007,** *129* (50), 15474-+.
28. Lienkamp, K.; Madkour, A. E.; Musante, A.; Nelson, C. F.; Nuesslein, K.; Tew, G. N., Antimicrobial polymers prepared by ROMP with unprecedented selectivity: A molecular construction kit approach. *J Am Chem Soc* **2008,** *130* (30), 9836-9843.
29. Palermo, E. F.; Kuroda, K., Chemical Structure of Cationic Groups in Amphiphilic Polymethacrylates Modulates the Antimicrobial and Hemolytic Activities. *Biomacromolecules* **2009,** *10* (6), 1416-1428.
30. Oda, Y.; Kanaoka, S.; Sato, T.; Aoshima, S.; Kuroda, K., Block versus Random Amphiphilic Copolymers as Antibacterial Agents. *Biomacromolecules* **2011,** *12* (10), 3581-3591.
31. Porel, M.; Brown, J. S.; Alabi, C. A., Sequence-Defined Oligothioetheramides. *Synlett* **2015,** *26* (5), 565-571.
32. Porel, M.; Thornlow, D. N.; Artim, C. M.; Alabi, C. A., Sequence-Defined Backbone Modifications Regulate Antibacterial Activity of OligoTEAs. *ACS Chem Biol* **2017,** *12* (3), 715-723.
33. Zhou, Z.; Ergene, C.; Lee, J. Y.; Shirley, D. J.; Carone, B. R.; Caputo, G. A.; Palermo, E. F., Sequence and Dispersity Are Determinants of Photodynamic Antibacterial Activity Exerted by Peptidomimetic Oligo(thiophene)s. *ACS Appl Mater Inter* **2019,** *11* (2), 1896-1906.
34. Appelt, C.; Wessolowski, A.; Soderhall, J. A.; Dathe, M.; Schmieder, P., Structure of the antimicrobial, cationic hexapeptide cyclo(RRWWRF) and its analogues in solution and bound to detergent micelles. *ChemBioChem* **2005,** *6* (9), 1654-1662.
35. Appelt, C.; Wessolowski, A.; Dathe, M.; Schmieder, P., Structures of cyclic, antimicrobial peptides in a membrane-mimicking environment define requirements for activity. *J Pept Sci* **2008,** *14* (4), 524-527.
36. Junkes, C.; Wessolowski, A.; Farnaud, S.; Evans, R. W.; Good, L.; Bienert, M.; Dathe, M., The interaction of arginine- and tryptophan-rich cyclic hexapeptides with Escherichia coli membranes. *J Pept Sci* **2008,** *14* (4), 535-543.

37. Falanga, A.; Nigro, E.; De Biasi, M. G.; Daniele, A.; Morelli, G.; Galdiero, S.; Scudiero, O., Cyclic Peptides as Novel Therapeutic Microbicides: Engineering of Human Defensin Mimetics. *Molecules* **2017,** *22* (7).
38. Mika, J. T.; Moiset, G.; Cirac, A. D.; Feliu, L.; Bardaji, E.; Planas, M.; Sengupta, D.; Marrink, S. J.; Poolman, B., Structural basis for the enhanced activity of cyclic antimicrobial peptides: The case of BPC194. *BBA-Biomembranes* **2011,** *1808* (9), 2197-2205.
39. Avedissian, S. N.; Liu, J. J.; Rhodes, N. J.; Lee, A.; Pais, G. M.; Hauser, A. R.; Scheetz, M. H., A Review of the Clinical Pharmacokinetics of Polymyxin B. *Antibiotics* **2019,** *8* (1).
40. Diep, J. K.; Covelli, J.; Sharma, R.; Ruszaj, D. M.; Kaye, K. S.; Li, J.; Straubinger, R. M.; Rao, G. G., Comparison of the composition and in vitro activity of polymyxin B products. *Int J Antimicrob Ag* **2018,** *52* (3), 365-371.
41. Velkov, T.; Roberts, K. D.; Nation, R. L.; Thompson, P. E.; Li, J., Pharmacology of polymyxins: new insights into an 'old' class of antibiotics. *Future Microbiol* **2013,** *8* (6), 711-724.
42. Porel, M.; Thornlow, D. N.; Phan, N. N.; Alabi, C. A., Sequence-defined bioactive macrocycles via an acid-catalysed cascade reaction. *Nature Chemistry* **2016,** *8* (6), 591-597.
43. Song, A. R.; Walker, S. G.; Parker, K. A.; Sampson, N. S., Antibacterial Studies of Cationic Polymers with Alternating, Random, and Uniform Backbones. *ACS Chem Biol* **2011,** *6* (6), 590-599.
44. Zhou, Z.; Palermo, E. F., Templated Ring-Opening Metathesis (TROM) of Cyclic Olefins Tethered to Unimolecular Oligo(thiophene)s. *Macromolecules* **2018,** *51* (15), 6127–6137.
45. Palermo, E. F.; Vemparala, S.; Kuroda, K., Cationic Spacer Arm Design Strategy for Control of Antimicrobial Activity and Conformation of Amphiphilic Methacrylate Random Copolymers. *Biomacromolecules* **2012,** *13* (5), 1632-1641.

TOC GRAPHIC